Proceedings of the 17th World Congress
The International Federation of Automatic Control
Seoul, Korea, July 6-11, 2008

Terrain Avoidance Model Predictive Control for Autonomous Rotorcraft

B. Guerreiro * **C. Silvestre** * **R. Cunha** *

* *Instituto Superior Técnico, Institute for Systems and Robotics*
Av. Rovisco Pais, 1, 1049-001 Lisboa, Portugal
(email: {bguerreiro,cjs,rita}@isr.ist.utl.pt)

Abstract: This paper presents a terrain avoidance control methodology for autonomous rotorcraft applied to low altitude flight. A model predictive control formulation is used to adequately address the terrain avoidance problem, which involves stabilizing a nonlinear highly coupled dynamic model, while avoiding collisions with the terrain and preventing input and state saturations. Computing the model predictive control law amounts to solving a finite horizon open-loop optimal control problem subject to the state difference equations that describe the rotorcraft nonlinear dynamic model. State and input saturations are added to the optimization cost functional as penalties and terrain avoidance is achieved by penalizing the distance between the vehicle and the closest point on the terrain, yielding smooth and collision-free trajectories. Simulation results, obtained with a simplified version of a small-scale helicopter nonlinear dynamic model, are presented to assess the performance of the methodology with different reference paths and terrain profiles, including the extreme case where a desired path leads to collision with the terrain.

Keywords: Obstacle avoidance; Helicopter control; Model predictive control.

1. INTRODUCTION

In this paper the problem of low altitude terrain avoidance flight for autonomous rotorcraft is addressed. Within the scope of Unmanned Aerial Vehicles, autonomous rotorcraft have been steadily growing as a major topic of research. They have the potential to perform high precision tasks in challenging and uncertain operation scenarios as new sensor technology and increasingly powerful computational systems are available. Missions like aerial surveillance, infrastructure automatic inspection or 3-D surface mapping in unknown environments demand highly adaptable autonomous vehicles that can meet low altitude flight requirements, thus emphasizing the importance of terrain avoidance strategies (e.g. Paulino et al. [2006]).

The presented methodology is formulated within the scope of model-based predictive control (MPC) in order to simultaneously solve the trajectory tracking and terrain avoidance problems. The control law is obtained by solving on-line, at each sampling instant, a finite horizon open-loop optimal control problem, using the current state of the plant as the initial state. The optimization yields an optimal control sequence and the first element of this sequence is applied to the plant. Since the optimal control problem is solved online, it is straightforward to add state and control saturation constraints as penalty functions to the cost functional. Moreover, the vehicle model constraint can be readily incorporated in the cost functional using lagrange multipliers. These are standard procedures in MPC literature such as Sutton and Bitmead [2000], Kim et al. [2002], Shim et al. [2003]. To implement the terrain avoidance capability, a virtual repulsive field is generated around the helicopter such that any obstacle within its range (possibly the terrain) is weighted in the optimal control cost functional, directing the vehicle trajectory away from collisions. Since this additional constraint is also included in the cost functional as a penalty function, the original constrained optimization problem is formulated as an unconstrained optimization problem.

The resulting optimization problem is numerically solved using the gradient and quasi-Newton methods to compute the search direction and using Wolfe's rule as the line search algorithm to solve the step size optimization subproblem (see Nocedal and Wright [1999]). The vehicle model considered in this work is a helicopter nonlinear dynamic model, derived from first-principles and specially suited for model-scale helicopters (see Cunha [2002], Cunha et al. [2005]). The control algorithm relies on a simplified version of the referred model to compute the sequence of state vectors given a sequence of input vectors.

This paper is organized as follows: Section 2 presents a brief summary of the helicopter dynamic model; Section 3 formulates the terrain avoidance MPC problem, describing the control problem, the saturation, terrain and model constraints, and the optimization algorithm; implementation issues and the simulation results are presented in Section 4 and finally Section 5 summarizes the main ideas of this paper and discusses directions for future work.

2. HELICOPTER MODEL

This section summarizes the helicopter dynamic model. A comprehensive coverage of helicopter flight dynamics can be found in Padfield [1996]. In Cunha [2002], Cunha et al.

978-1-1234-7890-2/08/$20.00 © 2008 IFAC 10.3182/20080706-5-KR-1001.1928

[2005] this model and its simplified version are described in more detail.

Consider the helicopter modeled as a rigid body dynamic where the resultant force and moment applied to the helicopter's center of mass is the sum of the contributions of the helicopter components and gravitational force. Let $({}^I\mathbf{p}_B, {}^I_BR) \in SE(3) \triangleq \mathbb{R}^3 \times SO(3)$ denote the configuration of the body frame $\{B\}$ (attached to the vehicle's center of mass) with respect to the inertial frame $\{I\}$. Consider also the Z-Y-X Euler angles $\boldsymbol{\lambda}_B = [\,\phi_B\ \theta_B\ \psi_B\,]'$, $\theta_B \in]-\frac{\pi}{2}, \frac{\pi}{2}[$, $\phi_B, \psi_B \in \mathbb{R}$, representing the orientation of $\{B\}$ relative to $\{I\}$ such that ${}^I_BR = \mathcal{R}(\boldsymbol{\lambda}_B)$. In addition, let $\mathbf{v}_B$ and $\boldsymbol{\omega}_B$ denote the linear and angular body velocities, respectively, where $\mathbf{v}_B = {}^B_IR\,{}^I\dot{\mathbf{p}}_B \in \mathbb{R}^3$, $\boldsymbol{\omega}_B = {}^B_IR\,{}^I\boldsymbol{\omega}_B$, and ${}^I\boldsymbol{\omega}_B$ is the angular velocity of $\{B\}$ relative to $\{I\}$. For the sake of simplicity, the subscripts and superscripts of the state variables $\mathbf{v}_B$, $\boldsymbol{\omega}_B$, ${}^I\mathbf{p}_B$ and $\boldsymbol{\lambda}_B$ are dropped, so that for example $\mathbf{p} = {}^I\mathbf{p}_B$.

Using this notation, the helicopter state equations, combining kinematics and dynamics, can be written as

$$\begin{cases} \dot{\mathbf{v}} = -\boldsymbol{\omega} \times \mathbf{v} + \frac{1}{m}\left[\mathbf{f}_h(\mathbf{v}, \boldsymbol{\omega}, \mathbf{u}) + \mathbf{f}_g(\phi, \theta)\right] \\ \dot{\boldsymbol{\omega}} = -I^{-1}(\boldsymbol{\omega} \times I\,\boldsymbol{\omega}) + I^{-1}\,\mathbf{n}_h(\mathbf{v}, \boldsymbol{\omega}, \mathbf{u}) \\ \dot{\mathbf{p}} = \mathcal{R}(\boldsymbol{\lambda})\,\mathbf{v} \\ \dot{\boldsymbol{\lambda}} = \mathcal{Q}(\phi, \theta)\,\boldsymbol{\omega} \end{cases}, \qquad (1)$$

where m is the vehicle mass, I is the tensor of inertia about the frame $\{B\}$, $\mathbf{u}$ is the input vector, $\mathbf{f}_h$ and $\mathbf{n}_h$ are the external force and moment vectors due to the helicopter components, and $\mathbf{f}_g$ is the gravitational force vector, all expressed in the body frame, and $\mathcal{Q}$ is the transformation from angular rates to Euler angle derivatives. The state vector $\mathbf{x} = [\mathbf{v}'\ \boldsymbol{\omega}'\ \mathbf{p}'\ \boldsymbol{\lambda}']' \in \mathcal{X} \subset \mathbb{R}^{n_x}$ has dimension $n_x = 12$. The input vector $\mathbf{u} \in \mathcal{U} \subset \mathbb{R}^{n_u}$ with $n_u = 4$, defined as $\mathbf{u} = [\,\theta_{c_0}\ \theta_{c_{1c}}\ \theta_{c_{1s}}\ \theta_{c_{0t}}\,]'$, comprises the main rotor collective input θ_{c_0}, the main rotor cyclic inputs $\theta_{c_{1c}}$ and $\theta_{c_{1s}}$, and the tail rotor collective input $\theta_{c_{0t}}$.

The force and moment vectors can be decomposed as $\mathbf{f}_h = \mathbf{f}_{mr} + \mathbf{f}_{tr} + \mathbf{f}_{fus} + \mathbf{f}_{tp} + \mathbf{f}_{fn}$ and $\mathbf{n}_h = \mathbf{n}_{mr} + \mathbf{n}_{tr} + \mathbf{n}_{fus} + \mathbf{n}_{tp} + \mathbf{n}_{fn}$, where the subscripts mr, tr, fus, tp and fn stand for main rotor, tail rotor, fuselage, horizontal tail plane and vertical tail fin, respectively.

2.1 Main Rotor

As the primary source of lift, propulsion and control, the main rotor dominates the helicopter dynamic behavior. As a result of the aerodynamic lift forces that are generated at the surface of its rotating blades, the main rotor is responsible for the helicopter's distinctive ability to operate in low-speed regimes, which include hovering and vertical maneuvering.

To present the main rotor equations of motion, two additional frames need to be introduced:

$\{hw\}$ – Hub/Wind frame. Non-rotating frame, with its origin at the hub, x-axis aligned with the component of the helicopter linear velocity relative to the fluid that is parallel with the hub plane;

$\{b\}$ – Blade frame. Coordinate frame attached to the blade, describing rotation, flapping, and pitching motions. The y-axis is aligned with the blade chord.

Most of the helicopter maneuvering capabilities result from effectively controlling the main rotor aerodynamic loads. This is achieved by means of the swashplate - a mechanism responsible for applying a different blade pitch angle θ_m at each blade azimuth angle ψ_m, such that $\theta_m(\psi_m) = \theta_{c_0} + \theta_{1c}\cos\psi_m + \theta_{1s}\sin\psi_m$. The collective command θ_{c_0} is directly applied to the main rotor blades, whereas the cyclics θ_{1c} and θ_{1s} result from combining the cyclic commands $\theta_{c_{1c}}$ and $\theta_{c_{1s}}$ with the flapping motion of the Bell-Hiller stabilizing bar, also called flybar. This combined motion can be described by the first order system

$$\begin{aligned} &\Omega\, A_{\dot{\theta}}\, \dot{\boldsymbol{\theta}}_1 + \Omega^2 A_\theta(\mu)\,\boldsymbol{\theta}_1 = \\ &= \Omega^2\left(B_\theta(\mu)\,\boldsymbol{\theta}_{c_1} + B_\omega\,\boldsymbol{\omega} + B_\lambda(\mu)\,\boldsymbol{\lambda}\right), \end{aligned} \qquad (2)$$

where $\boldsymbol{\theta}_1 = [\,\theta_{1c}\ \theta_{1s}\,]'$, $\boldsymbol{\theta}_{c_1} = [\,\theta_{c_{1c}}\ \theta_{c_{1s}}\,]'$, $\boldsymbol{\omega} = [\,\bar{p}\ \bar{q}\,]'$, $\boldsymbol{\lambda} = [\,\mu_z - \lambda_0\ \lambda_{1c}\ \lambda_{1s}\,]'$ and $\Omega = \dot{\psi}_m$ is the rotor speed. The variables μ and μ_z are the normalized x and z-components of the hub linear velocity and $\bar{p}$ and $\bar{q}$ are the normalized x and y-components of the angular velocity, all expressed in the frame $\{hw\}$. Detailed expressions for the matrices $A_{\dot{\theta}}$, $A_\theta(\mu)$, $B_\theta(\mu)$, B_ω, and $B_\lambda(\mu)$ can be found in Cunha et al. [2005]. Due to this additional dynamic component, the augmented state vector becomes $\mathbf{x} = \left[\,\mathbf{v}'\ \boldsymbol{\omega}'\ \mathbf{p}'\ \boldsymbol{\lambda}'\ \boldsymbol{\theta}_1'\,\right]'$ and $n_x = 14$.

As result of the thrust force generated at the surface of the rotating blades, the air is accelerated downwards creating a flowfield, usually called induced downwash. The downwash can be decomposed in Fourier Series and approximated by the constant and first-order harmonic terms, yielding an expression similar to that of the blade pitch angle $\lambda(\psi_m) = \lambda_0 + r_m(\lambda_{1c}\cos\psi_m + \lambda_{1s}\sin\psi_m)$, where r_m is the rotor radius integration variable. Also as a consequence of the rotation and feathering (blade pitching) motions and interaction with the motion of the helicopter, the blades describe flap and lag motions, roughly characterized by pulling up and backwards, respectively, the tip of the blade. In this work, assuming that the blades are assumed rigid and linked to the hub through flap hinge springs with stiffness k_β, the lag motion is neglected and the flap motion is approximated by the first three components of the Fourier Series expansion of the steady-state solution, that is,

$$\boldsymbol{\beta} = A_0^{-1}(\mu)\left[B_1(\mu)\,\boldsymbol{\theta} + B_2(\mu)\,\boldsymbol{\omega} + B_3(\mu)\,\boldsymbol{\lambda}\right], \qquad (3)$$

where $\boldsymbol{\beta} = [\,\beta_0\ \beta_{1c}\ \beta_{1s}\,]'$, $\boldsymbol{\theta} = [\,\theta_{c_0}\ \theta_{1c}\ \theta_{1s}\,]'$, and the matrices $A_0(\mu)$, $B_1(\mu)$, $B_2(\mu)$, and $B_3(\mu)$ are defined in Cunha et al. [2005].

The forces and moments generated by the main rotor are the sum of the contributions of each blade expressed in the hub frame. The main rotor contribution to the total force acting on the helicopter can be written as $\mathbf{f}_{mr} = {}^B_{hw}R\,{}^{hw}\mathbf{f}_{mr}$, with the expression for ${}^{hw}\mathbf{f}_{mr}$ given by

$${}^{hw}\mathbf{f}_{mr} \simeq \frac{n_b}{2}\begin{bmatrix} -Y_{1s} \\ -Y_{1c} \\ 2\,Z_0 \end{bmatrix} + \frac{n_b}{2}\begin{bmatrix} -Z_{1c} & -Z_0 - \dfrac{Z_{2c}}{2} & -\dfrac{Z_{2s}}{2} \\ Z_{1s} & \dfrac{Z_{2s}}{2} & Z_0 - \dfrac{Z_{2c}}{2} \\ 0 & 0 & 0 \end{bmatrix}\boldsymbol{\beta}$$

where n_b is the number of blades, $Y_{(.)}$ and $Z_{(.)}$ are the components of the Fourier Series decomposition of the aerodynamic force generated at each blade. Similarly, the main rotor contribution to the overall moment is computed using $\mathbf{n}_{mr} = {}^{B}_{hw}R\,{}^{hw}\mathbf{n}_{mr}$, where the expression for ${}^{hw}\mathbf{n}_{mr}$ can be rewritten as

$$ {}^{hw}\mathbf{n}_{mr} \simeq n_b \begin{bmatrix} 0 \\ 0 \\ N_0 \end{bmatrix} + \tfrac{n_b}{2} \begin{bmatrix} -N_{1c} & -N_0 - \dfrac{N_{2c}}{2} & -k_\beta - \dfrac{N_{2s}}{2} \\ N_{1s} & -k_\beta + \dfrac{N_{2s}}{2} & N_0 - \dfrac{N_{2c}}{2} \\ 0 & 0 & 0 \end{bmatrix} \boldsymbol{\beta} $$

where $N_{(.)}$ are the components of the Fourier Series decomposition of the aerodynamic yaw moment generated at each blade.

2.2 The Other Components

The tail rotor, placed at the tail boom in order to counteract the moment generated by the rotation of the main rotor, provides yaw control of the helicopter. To model this component we can use the same principles adopted for the main rotor, neglecting the blade flapping and pitching motions, which have little significance due to the small rotor size. The tail rotor contribution to the total force can be approximated by

$$ \mathbf{f}_{tr} = {}^{B}_{tr}R\,{}^{tr}\mathbf{f} \simeq \begin{bmatrix} 0 \\ -n_{b_t} Z_{0_t} \\ 0 \end{bmatrix} , \tag{4} $$

where n_{b_t} is the number of blades of the tail rotor, Z_{0_t} is the thrust force produced by the tail rotor and ${}^{B}_{tr}R^{\,tr}$ is the rotation from the tail rotor frame $\{tr\}$ to the body frame $\{B\}$. Similarly, the moment expression is given by

$$ \mathbf{n}_{tr} = \begin{bmatrix} 0 \\ -n_{b_t} N_{0_t} \\ 0 \end{bmatrix} + {}^{B}\mathbf{p}_{tr} \times \mathbf{f}_{tr} , \tag{5} $$

where N_{0_t} is the tail rotor generated torque.

Accurately modeling of the aerodynamic forces and moments generated by the flow surrounding the helicopter fuselage is a demanding task. In this work these loads are modeled as functions of the mean flow speed v_{fus}, the incidence angle α_{fus} and the sideslip angle β_{fus}. The horizontal tail plane and vertical tail fin are modeled as normal wings, whose aerodynamic force contributions can be approximated by functions of the angle of attack and sideslip, respectively.

3. MODEL PREDICTIVE CONTROL PROBLEM

In this section the Model Predictive Control problem is formulated as a discrete-time open-loop optimal control problem with finite horizon, subject to the discretized nonlinear model equations, the state and input saturation constraints, and the terrain avoidance constraint.

In general, the vehicle dynamics can be modeled as a continuous-time state-space differential equation

$$ \dot{\mathbf{x}}(t) = \mathbf{f}_c\left(\mathbf{x}(t), \mathbf{u}(t)\right) , \tag{6} $$

where $\mathbf{x} \in \mathcal{X}$ and $\mathbf{u} \in \mathcal{U}$, noting that $\mathcal{X} \subset \mathbb{R}^{n_x}$ and $\mathcal{U} \subset \mathbb{R}^{n_u}$ denote the feasibility sets of the state and control vectors, respectively. Since the control problem is formulated as a discrete-time open loop optimal control problem, the helicopter motion needs to be described as a difference equation, which can be obtained from

$$ \begin{aligned} \mathbf{x}((k+1)T_s) &\approx \mathbf{x}(kT_s) + T_s \mathbf{f}_c\left(\mathbf{x}(kT_s), \mathbf{u}(kT_s)\right) \\ &= \mathbf{f}\left(\mathbf{x}(k\,T_s), \mathbf{u}(k\,T_s)\right) , \end{aligned} \tag{7} $$

where T_s is the sample time. Using a compact notation, the previous equation can be rewritten as

$$ \mathbf{x}_{k+1} \approx \mathbf{f}\left(\mathbf{x}_k, \mathbf{u}_k\right) . \tag{8} $$

Let N be the prediction horizon of the control problem, $U_k = \{\mathbf{u}_k, \ldots, \mathbf{u}_{k+N-1}\}$ the sequence of control inputs at iteration k, and $X_k = \{\mathbf{x}_k, \ldots, \mathbf{x}_{k+N}\}$ the sequence of state vector generated by that control sequence. The saturation constraints of the state and input sequences are defined by the conditions $X_k \in \boldsymbol{\mathcal{X}}_N$ and $U_k \in \boldsymbol{\mathcal{U}}_N$, where $\boldsymbol{\mathcal{X}}_N = \{X_k : \mathbf{x}_i \in \mathcal{X}, \forall_{i=k,\ldots,k+N}\}$ and $\boldsymbol{\mathcal{U}}_N = \{U_k : \mathbf{u}_i \in \mathcal{U}, \forall_{i=k,\ldots,k+N-1}\}$. Let $\bar{X}_k \in \boldsymbol{\mathcal{X}}_N$ and $\bar{U}_k \in \boldsymbol{\mathcal{U}}_N$ be the reference state sequence and the respective control sequence, chosen to satisfy the saturation constraints. The errors between the actual and desired state and input vectors are defined as $\tilde{\mathbf{x}}_i = \mathbf{x}_i - \bar{\mathbf{x}}_i$, and $\tilde{\mathbf{u}}_i = \mathbf{u}_i - \bar{\mathbf{u}}_i$, respectively.

Using (8), the model constraint for N steps ahead horizon can be written as

$$ F_M(X_k, U_k) = \begin{bmatrix} \mathbf{f}(\mathbf{x}_k, \mathbf{u}_k) - \mathbf{x}_{k+1} \\ \vdots \\ \mathbf{f}(\mathbf{x}_{k+N-1}, \mathbf{u}_{k+N-1}) - \mathbf{x}_{k+N} \end{bmatrix} = 0 \tag{9} $$

whereas the terrain constraint is denoted by

$$ F_T(X_k) = \left[\, f_T(\mathbf{x}_k) \;\cdots\; f_T(\mathbf{x}_{k+N}) \,\right]' = 0 , \tag{10} $$

where $f_T(.)$ weights the distance between the vehicle and the terrain, as discussed later on this section.

Given this set of constraints, the terrain avoidance MPC problem can be defined as

$$ \begin{aligned} U_k^* &= \arg\min_{U_k} J_k && (11) \\ s.t. \quad & X_k \in \boldsymbol{\mathcal{X}}_N \ , \ U_k \in \boldsymbol{\mathcal{U}}_N && (12) \\ & F_M(X_k, U_k) = 0 && (13) \\ & F_T(X_k) = 0 && (14) \end{aligned} $$

where

$$ J_k = J(X_k, \bar{X}_k, U_k, \bar{U}_k) = F_{k+N} + \sum_{i=k}^{k+N-1} L_i , \tag{15} $$

$$ F_i = F(\mathbf{x}_i, \bar{\mathbf{x}}_i) = \tfrac{1}{2}\, \tilde{\mathbf{x}}_i'\, P\, \tilde{\mathbf{x}}_i , \tag{16} $$

$$ L_i = L(\mathbf{x}_i, \bar{\mathbf{x}}_i, \mathbf{u}_i, \bar{\mathbf{u}}_i) = \tfrac{1}{2}\, [\tilde{\mathbf{x}}_i'\, Q\, \tilde{\mathbf{x}}_i + \tilde{\mathbf{u}}_i'\, R\, \tilde{\mathbf{u}}_i] \tag{17} $$

and P, Q, and R are symmetric positive definite matrices. In summary, the objective of the terrain avoidance MPC problem is to find, at each iteration k, the optimal control sequence U_k^* with horizon N, such that the resulting state sequence X_k^* follows the state reference $\bar{X}_k$ without violating the state and input constraints imposed by (12) and avoiding collisions by verifying (14).

Following the standard approach, the constrained optimization problem presented above can be solved by reformulating it as an unconstrained optimization problem and using gradient methods to approximate the optimal solution. While constraint (13) is eliminated using lagrange multipliers, constraints (12) and (14) are incorporated into the cost functional resorting to penalty methods. In the following subsections each constraint function and the way they are included in the unconstrained optimization cost functional are described.

3.1 Terrain Avoidance Constraint

The goal is to define a terrain constraint function in the form of (10), such that the helicopter finds the best collision free trajectory even if the reference trajectory goes through the terrain. This constraint can be implemented by defining a repulsive field around the helicopter (a sphere with radius r_S), and weighting exponentially the minimum distance between the helicopter position $\mathbf{p}$ and the closest terrain point $\mathbf{p}_m$. Considering the position error vector between these two points $\mathbf{p}_e = \mathbf{p} - \mathbf{p}_m$, the sphere can be defined as $\mathbf{p}_e' \, \mathbf{p}_e = r_S^2$. Noting that the closest terrain point is a function of the position of the helicopter $\mathbf{p}_m(\mathbf{p})$, a function $g(\mathbf{x})$ that measures the distance between the terrain and the sphere, depending only on the state vector, can be defined as

$$g\left(\mathbf{x}\right) = \mathbf{p}_e' \, \mathbf{p}_e - r_S^2 \ , \tag{18}$$

such that $g\left(\mathbf{x}\right) = 0$ when the terrain touches the sphere. Thus, the terrain avoidance constraint function can be written as

$$f_T(\mathbf{x}) = e^{-g(\mathbf{x})} \ . \tag{19}$$

Since this function has always a positive value, the zero value is forced whenever the helicopter-terrain distance is greater than a predefined outer radius r_O where the influence of the terrain is negligible, that is $f_T = 0$ if $\|\mathbf{p}_e\| > r_O$.

3.2 State and Input Saturation Constraint

The state and input saturation constraint (12) can be incorporated in the cost functional as a penalty function $\mathbf{f}_R\left(\mathbf{x}, \mathbf{u}\right)$. This function has zero value if $\mathbf{x} \in \mathcal{X}$ and $\mathbf{u} \in \mathcal{U}$, and behaves as a quadratic function outside these sets. Assuming that the valid sets for state and input vectors are given by $\mathcal{X} = \{\mathbf{x} \in \mathbb{R}^{n_x} : |x^{(j)}| \leq x_{\max}^{(j)} \ \forall_{j=1,\ldots,n_x}\}$ and $\mathcal{U} = \{\mathbf{u} \in \mathbb{R}^{n_u} : |u^{(l)}| \leq u_{\max}^{(l)} \ \forall_{l=1,\ldots,n_u}\}$, respectively, the penalty function can be defined as

$$\begin{aligned}\mathbf{f}_R\left(\mathbf{x}, \mathbf{u}\right) =& \frac{1}{2}\sum_{j=1}^{n_x} h(|x^{(j)}| - x_{\max}^{(j)})^2 w_x^{(j)} \\ &+ \frac{1}{2}\sum_{l=1}^{n_u} h(|u^{(l)}| - u_{\max}^{(l)})^2 w_u^{(l)},\end{aligned} \tag{20}$$

where

$$h(a) = \begin{cases} a & \text{, if } a > 0 \\ 0 & \text{, otherwise} \end{cases} \tag{21}$$

and $w_x^{(j)}$ and $w_u^{(l)}$ are positive scalar weights. The partial derivatives of the terrain function are given by

$$\frac{\partial \mathbf{f}_R}{\partial x^{(j)}} = \text{sign}(x^{(j)}) h(|x^{(j)}| - x_{\max}^{(j)}) w_x^{(j)} \ , \tag{22}$$

$$\frac{\partial \mathbf{f}_R}{\partial u^{(l)}} = \text{sign}(u^{(l)}) h(|u^{(l)}| - u_{\max}^{(l)}) w_u^{(l)} \ . \tag{23}$$

3.3 Unconstrained Optimization Problem

Adding to the optimization cost functional the state and input saturation constraint and also the terrain avoidance constraint, the new problem can be written as

$$U_k^* = \arg\min_{U_k} \bar{J}_k \tag{24}$$

$$s.t. \quad F_M(X_k, U_k) = 0 \tag{25}$$

where

$$\bar{J}_k = \bar{J}(X_k, \bar{X}_k, U_k, \bar{U}_k) = \bar{F}_{k+N} + \sum_{i=k}^{k+N-1} \bar{L}_i \ , \tag{26}$$

$$\bar{F}_i = \bar{F}(\mathbf{x}_i, \bar{\mathbf{x}}_i) = F_i + \mathbf{f}_R(\mathbf{x}_i, 0) + \mathbf{f}_T(\mathbf{x}_i) \ , \tag{27}$$

$$\bar{L}_i = \bar{L}(\mathbf{x}_i, \bar{\mathbf{x}}_i, \mathbf{u}_i, \bar{\mathbf{u}}_i) = L_i + \mathbf{f}_R(\mathbf{x}_i, \mathbf{u}_i) + \mathbf{f}_T(\mathbf{x}_i) \ . \tag{28}$$

To solve the model constraint (25), the elimination method using Lagrange multipliers is used. Introducing the Lagrange multiplier sequence $\Lambda_k = \{\boldsymbol{\lambda}_{k+1}, \ldots, \boldsymbol{\lambda}_{k+N}\}$ and the Hamiltonian

$$H_i = H\left(\mathbf{x}_i, \mathbf{u}_i, \bar{\mathbf{x}}_i, \bar{\mathbf{u}}_i\right) = \bar{L}_i + \boldsymbol{\lambda}_{i+1}' \, \mathbf{f}_d\left(\mathbf{x}_i, \mathbf{u}_i\right) \ , \tag{29}$$

the cost functional $\bar{J}$ can be redefined adding a zero value sequence, that is,

$$\bar{J}_k = \bar{F}_{k+N} - \boldsymbol{\lambda}_{k+N}' \, \mathbf{x}_{k+N} + \sum_{i=k+1}^{k+N-1} \left[H_i - \boldsymbol{\lambda}_i' \, \mathbf{x}_i\right] + H_k. \tag{30}$$

For a fixed initial state $\mathbf{x}_k$, the first order condition of optimality yield

$$\frac{\partial \bar{J}_k}{\partial \mathbf{x}_i} = \frac{\partial H_i}{\partial \mathbf{x}_i} - \boldsymbol{\lambda}_i = 0 \ , \ \forall_{i=k+1,\ldots,k+N-1} \ , \tag{31}$$

$$\frac{\partial \bar{J}_k}{\partial \mathbf{x}_{k+N}} = \frac{\partial \bar{F}_{k+N}}{\partial \mathbf{x}_{k+N}} - \boldsymbol{\lambda}_{k+N} = 0 \ , \tag{32}$$

$$\frac{\partial \bar{J}_k}{\partial \mathbf{u}_i} = \frac{\partial H_i}{\partial \mathbf{u}_i} = 0 \ , \ \forall_{i=k,\ldots,k+N-1} \ . \tag{33}$$

where $\frac{\partial H_i}{\partial \mathbf{u}_i} = \frac{\partial \bar{L}_i}{\partial \mathbf{u}_i} + \frac{\partial \mathbf{f}_{d_i}}{\partial \mathbf{u}_i}\boldsymbol{\lambda}_{i+1}$ and $\frac{\partial H_i}{\partial \mathbf{x}_i} = \frac{\partial \bar{L}_i}{\partial \mathbf{x}_i} + \frac{\partial \mathbf{f}_{d_i}}{\partial \mathbf{x}_i}\boldsymbol{\lambda}_{i+1}$. Since the Lagrange multipliers sequence is multiplying zero value terms, they can be arbitrarily chosen. In particular, by choosing

$$\boldsymbol{\lambda}_{k+N} = \frac{\partial \bar{F}_{k+N}}{\partial \mathbf{x}_{k+N}} \text{ and } \boldsymbol{\lambda}_i = \frac{\partial H_i}{\partial \mathbf{x}_i}, \ \forall_{i=k+1,\ldots,k+N-1}, \tag{34}$$

the first order conditions of optimality reduce to (33).

Following the standard approach, an iterative algorithm based on the first order gradient method can be applied to estimate U_k^*, whereby at each iteration j, the control sequence is updated according to

$$U_k^{(j+1)} = U_k^{(j)} + s^{(j)} \, \Delta_k^{(j)} \tag{35}$$

where the step size is denoted by $s^{(j)}$ and the search direction by $\Delta_k^{(j)}$. The optimization algorithm can be summarized as follows.

Algorithm 1. Minimization algorithm for the MPC unconstrained problem.

```
(1) Initialize $X_k^{(0)}$, $\bar{X}_k$, $U_k^{(0)}$ and $\bar{U}_k$ and set $j = 0$;
(2) Compute $\{\boldsymbol{\lambda}_i\}$ using (34), $i = k+N, \ldots, k$;
(3) Compute $\left\{\frac{\partial H_i}{\partial \mathbf{u}_i}\right\}$, $i = k, \ldots, k+N-1$;
(4) Compute the search direction $\Delta_k^{(j)}$ ;
(5) Compute the step size $s^{(j)}$ using Wolfe's rule;
(6) Compute $U_k^{(j+1)}$ using (35) and $X_k^{(j+1)} = \{\mathbf{x}_i\}$ using
    $\mathbf{x}_{i+1} = \mathbf{f}_d\left(\mathbf{x}_i, \mathbf{u}_i\right)$, for $i = k+1, \ldots, k+N$;
(7) Test $\|\nabla \bar{J}_k^{(j)}|_{(j)}\| < \varepsilon$: if false set $j = j+1$ and go to
    step (2), if true let $\hat{U}_k = U_k^{(j+1)}$ be the final estimate
    and continue;
```

(8) Apply first input vector $\hat{\mathbf{u}}_k$ to system and set the next initial solution to $U^{(0)}_{k+1} = \{\hat{\mathbf{u}}_{k+1}, \ldots, \hat{\mathbf{u}}_{k+N-1}\}$.

The search direction can be obtained using the gradient method, such that

$$\Delta^{(j)}_k = -\frac{\partial \mathbf{H}^{(j)}_k}{\partial U^{(j)}_k} \tag{36}$$

where $\mathbf{H}^{(j)}_k$ is the sequence of the Hamiltonian functions $H^{(j)}_i$ for $i = k, \ldots, k+N-1$ or using the quasi-Newton method, such that

$$\Delta^{(j)}_k = -D^{(j)}\,\frac{\partial \mathbf{H}^{(j)}_k}{\partial U^{(j)}_k} \tag{37}$$

where $D^{(j)}$ is an estimate of the inverse matrix of the second-order derivative of the Hamiltonian, given by

$$D^{(j+1)} = D^{(j)} + \frac{p\,p'}{p'\,q} + \frac{D^{(j)}\,q\,q'\,D^{(j)}}{q'\,D^{(j)}\,q} + \xi\,\tau\,v\,v' \tag{38}$$

with $p = U^{(j+1)}_k - U^{(j)}_k$, $q = \frac{\partial \mathbf{H}^{(j+1)}_k}{\partial U^{(j+1)}_k} - \frac{\partial \mathbf{H}^{(j)}_k}{\partial U^{(j)}_k}$, $v = \frac{p}{p'\,q} - \frac{D^{(j)}\,q}{\tau}$, $\tau = q'\,D^{(j)}\,q$ and $0 \leq \xi \leq 1$.

The line search optimization subproblem is numerically solved using the Wolfe conditions (see Nocedal and Wright [1999] for further details). Consider the step size optimization subproblem defined by

$$s^{(j)} = \arg\min_{s \geq 0} \phi(s)\ ; \tag{39}$$

where $\phi(s) = \bar{J}^{(j+1)}_k = \bar{J}_k\left(X^{(j+1)}_k, U^{(j+1)}_k\right)$, with $U^{(j+1)}_k$ given by (35). Let the derivative of $\phi(s)$ be given by

$$\phi'(s) = \frac{d\,\phi(s)}{ds} = \frac{d\,\bar{J}^{(j+1)}_k}{ds}$$

where $\frac{d\,\bar{J}^{(j+1)}_i}{ds} = \frac{\partial\,\bar{L}^{(j+1)}_i}{\partial \mathbf{x}'^{(j+1)}_i}\,\eta_i + \frac{\partial\,\bar{L}^{(j+1)}_i}{\partial \mathbf{u}'^{(j+1)}_i}\,\Delta^{(j)}_i + \frac{d\,\bar{J}^{(j+1)}_{i+1}}{ds}$, with $\frac{d\,\bar{J}^{(j+1)}_{k+N}}{ds} = \frac{\partial\,\bar{L}^{(j+1)}_{k+N}}{\partial \mathbf{x}'^{(j+1)}_{k+N}}\,\eta_{k+N}$ and $\eta_i = \frac{d\,\mathbf{x}'^{(j+1)}_i}{ds} = \frac{\partial\,\mathbf{f}^{(j+1)}_{i-1}}{\partial x^{(j+1)}_{i-1}}\,\eta_{i-1} + \frac{\partial\,\mathbf{f}^{(j+1)}_{i-1}}{\partial u^{(j+1)}_{i-1}}\,\Delta^{(j)}_{i-1}$.

Let also $\mu_i = \phi(0) + \sigma\,\phi'(0)\,s_i$ and $\mu_0 = \lambda\,\phi'(0)$, where σ and λ are parameters of the search algorithm. The Wolfe rule classifies the step size according to the sets

$$\begin{array}{l} \mathcal{A} = \{s_i > 0 : \phi(s_i) \leq \mu_i\ \wedge\ \phi'(s_i) \geq \mu_0\} \\ \mathcal{D} = \{s_i > 0 : \phi(s_i) > \mu_i\} \\ \mathcal{E} = \{s_i > 0 : \phi(s_i) \leq \mu_i\ \wedge\ \phi'(s_i) < \mu_0\} \end{array} \tag{40}$$

that define the acceptable, the right unacceptable and the left unacceptable step sizes, respectively. The algorithm that finds an acceptable step size, i.e. an estimate of the optimal step size, is given below.

Algorithm 2. Line search algorithm using Wolfe's rule.

```
(1) Initialize $s_0 > 0$, $e = 0$, $d = +\infty$ and $i = 0$;
(2) test $s_i$: if $s_i \in \mathcal{A}$ set $s^{(j)} = s_i$ and stop; if $s_i \in \mathcal{D}$ set
    $d = s_i$; if $s_i \in \mathcal{E}$ set $e = s_i$;
(3) test $d$: if $d = +\infty$ choose $s_{i+1} > s_i$; if $d < +\infty$: choose
    $s_{i+1} \in (e, d)$;
(4) $i \leftarrow i + 1$ and return to step 2;
```

4. SIMULATION RESULTS

The Terrain Avoidance MPC method is designed to provide low altitude flight capabilities even for scenarios where the predefined trajectory collides with the terrain. In this section the performance of the terrain avoidance MPC method is evaluated in simulation.

Since the problem of terrain acquisition and representation is not the focus of this paper, it is assumed that the terrain is represented by an elevation function and that this information enters the control algorithm in the computation of the closest helicopter-terrain distance. In the results presented hereafter, the helicopter model described in Section 2 is parameterized for the Vario X-treme model scale helicopter and used to close the simulation loop. A simplified version of this model is used in the control algorithm, in order to efficiently compute the actuation at each sampling time. The simulations where carried out in an Intel Pentium Centrino processor at 1.7 GHz, using Matlab/Simulink with C mex-functions.

The terrain is represented by an elevation function that resembles a winding river stream and the reference trajectory is composed by 1) a hovering stage at the initial position; 2) a forward flight trajectory with constant speed $\|\mathbf{v}\| = 2m/s$; and 3) a hovering stage at the final position. The sample time is $T_s = 0.02s$ and the horizon is 70 sample times, or equivalently 1.4 seconds. This horizon allows the algorithm to predict impacts with the terrain and change the trajectory to avoid it. The precision of the solution is determined by the algorithm stop condition given by $\|\nabla \bar{J}^{(j)}_k|_{U^{(j)}_k}\| / \|\nabla \bar{J}^{(0)}_k|_{U^{(0)}_k}\| < 10^{-2}$.

The simulation results are presented in Figure 1, where the 3-D trajectory described by the helicopter and the time evolution of the position and actuation are shown. The average number of iterations for the quasi-Newton method with line search is 99.1 iterations, while the gradient method with line search required in average 135.5 iterations to complete a minimization. The usage of the line search algorithm allows the dramatic reduction of 40 times the average number of iterations, while the quasi-Newton method introduces a 30% reduction. The results shown are obtain with the quasi-Newton method, since the different methods yield similar results. According to these results, the control algorithm achieves effective terrain avoidance, changing the trajectory of the vehicle in order to avoid the terrain while keeping the vehicle the closest possible to the reference trajectory.

5. CONCLUSIONS

Motivated by the use of autonomous rotorcraft in low altitude flight applications, this paper presented a MPC-based strategy for terrain avoidance and motion control of helicopters. In addition to imposing state and input saturation constraints, the proposed solution enforces terrain avoidance by defining a repulsive field around the helicopter that grows exponentially as the distance between the vehicle and the closest point on the terrain decreases.

Following the standard approach in MPC literature, the constrained optimization problem was reformulated as an unconstrained optimization problem using the penalty

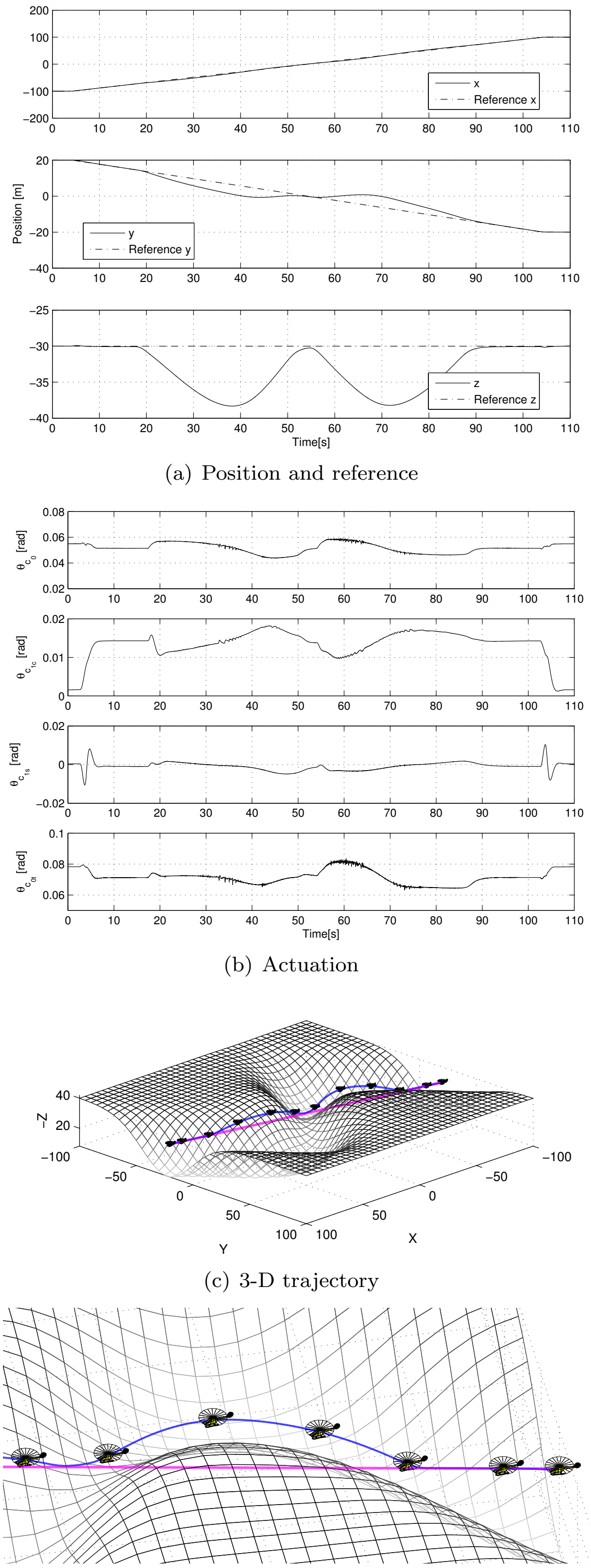

(a) Position and reference

(b) Actuation

(c) 3-D trajectory

(d) 3-D trajectory detail

Fig. 1. Trajectory tracking with terrain avoidance.

method to accommodate the saturation and terrain constraints and lagrange multipliers to eliminate the helicopter dynamic model constraint. The optimization problem was then solved using an iterative algorithm that relies on the gradient and quasi-Newton methods to find the search direction and the Wolfe rule to find an estimate of the optimal step size. The simulation results were obtained using a simplified nonlinear helicopter model in the MPC algorithm and the full model as the real plant, showing that the presented methodology can achieve effective terrain avoidance while steering the vehicle along a reference trajectory.

The proposed methodology, as most of the strategies using MPC in high sampling rate platforms, faces the challenge of real time implementation. The most CPU time consuming tasks involve the helicopter model computations and finding the closest terrain point. Hence, future work will deal with the simplification of the helicopter model and with the redefinition of the terrain representation in order to simplify the closest point computation. In addition, further effort shall be put on analyzing the influence of reducing the sampling frequency and the prediction horizon of the controller.

ACKNOWLEDGEMENTS

This work was partially supported by Fundação para a Ciência e a Tecnologia (ISR/IST pluriannual funding) through the POS Conhecimento Program that includes FEDER funds and by the PTDC/EEA-ACR/72853/2006 HELICIM project. The work of Bruno Guerreiro was supported by the PhD Student Grant SFRH/BD/21781/2005 from the Portuguese FCT POCTI programme.

REFERENCES

Rita Cunha. Modeling and control of an autonomous robotic helicopter. Master's thesis, Department of Electrical and Computer Engineering, Instituto Superior Técnico, Lisbon, Portugal, May 2002.

Rita Cunha, Bruno Guerreiro, and Carlos Silvestre. Vario-xtreme helicopter nonlinear model: Complete and simplified expressions. Technical report, Instituto Superior Técnico, Institute for Systems and Robotics, 2005.

H. Kim, D. Shim, and S. Sastry. Nonlinear model predictive tracking control for rotorcraft-based unmanned aerial vehicles. In *American Control Conference*, volume 5, pages 3576–3581, Anchorage, AK, May 2002.

Jorge Nocedal and Stephen Wright. *Numerical Optimization*. Springer Series in Operation Reasearch. Springer, 1999.

Gareth D. Padfield. *Helicopter Flight Dynamics: The Theory and Application of Flying Qualities and Simulation Modeling*. AIAA Education Series. AIAA, Washington DC, 1996.

N. Paulino, C. Silvestre, and R. Cunha. Affine parameter-dependent preview control for rotorcraft terrain following. *AIAA Journal of Guidance, Control, and Dynamics*, 29(6):1350–1359, 2006.

D. Shim, H. Kim, and S. Sastry. Decentralized reflective model predictive control of multiple flying robots in dynamic environment. *Conference on Decision and Control*, 2003. U.S.A.

G. Sutton and R. Bitmead. Computational implementation of nonlinear model predictive control to nonlinear submarine. In F. Allgöwer and A. Zheng, editors, *Nonlinear Model Predictive Control*, volume 26 of *Progress in Systems and Control Theory*, pages 461–471. Birkhäuser Verlag, Basel-Boston-Berlin, 2000.